

Figure 1. CAM proteins are partly co-transported in hippocampal neurons.

(A) Co-expression of $\beta 2\text{Na}_v\text{-GFP}$ and Nfasc186-mCherry, $\beta 1\text{Na}_v\text{-mCherry}$ or APP-mCherry in hippocampal neurons at 17 DIV. Yellow tracks indicate axonal co-transport while tracks in red (mCherry) or green (GFP) show individual transport for these markers at 17 DIV. Mean number of puncta along the axon (B) and their distribution as moving or stationary structures (C). (D) Distribution of co-labeled puncta per categories. Data are mean \pm SEM; $n=17$ to 22 neurons per condition from $n=3$ independent experiments. One-way analysis of variance with Tukey's post-hoc test (B; C, *, $p < 0.05$; **, $p < 0.01$; and ***, $p < 0.001$). The difference of distribution between proteins across all types of movement (D) was assessed using Chi-squared test (see Table S2 for exact p -values).

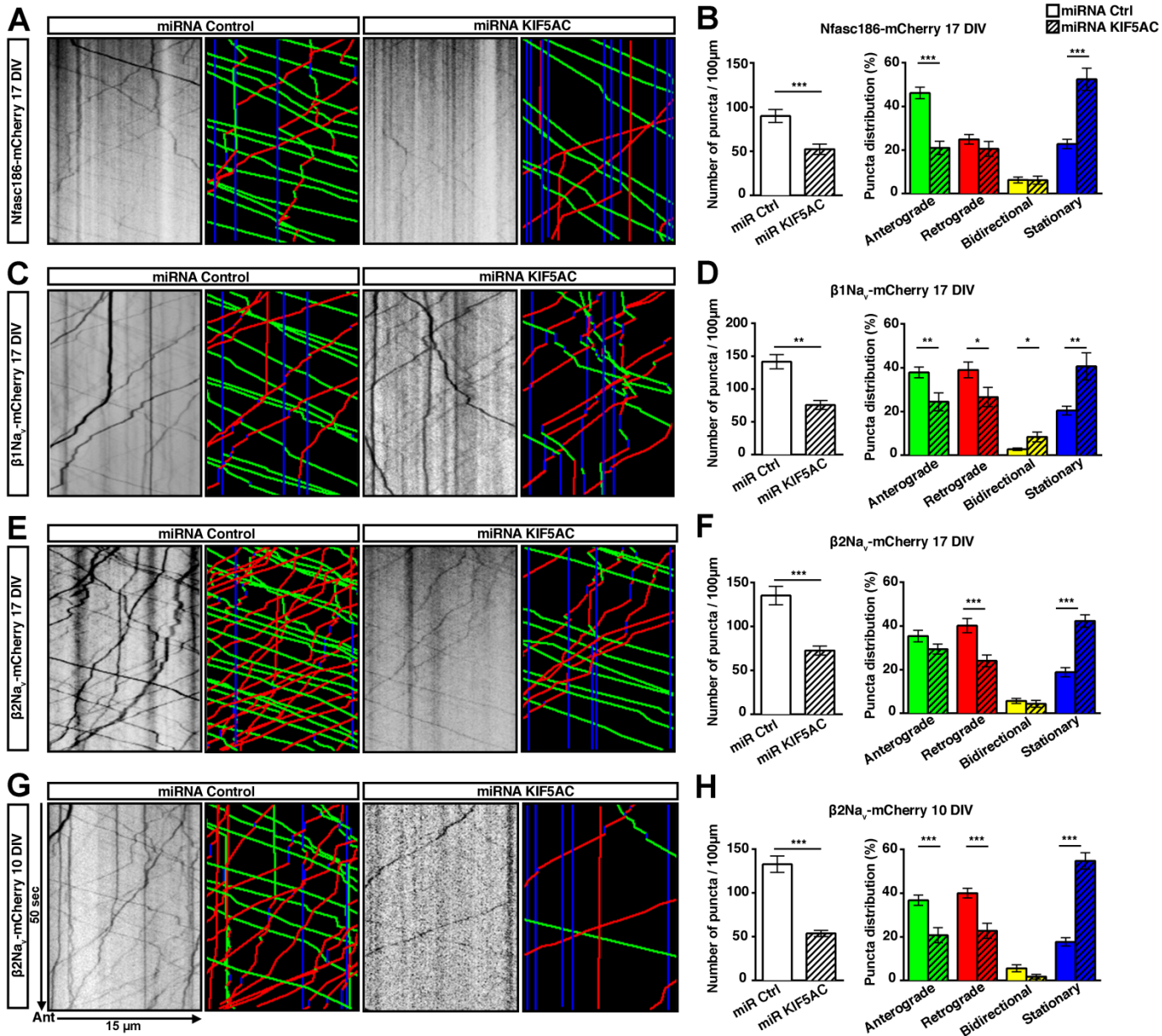


Figure 2. KIF5A and C participate in axonal transport of early cluster CAMs.

Hippocampal mixed cultures were co-transfected with control or KIF5AC miRNA together with Nfasc186-mCherry (A, B), $\beta 1\text{Na}_v\text{-mCherry}$ (C, D) or $\beta 2\text{Na}_v\text{-mCherry}$ (17 DIV: E, F; 10 DIV: G, H) expressing constructs. (A, C, E, G) Kymographs and corresponding tracks. (B, D, F, H) Mean number of puncta and distribution analysis of nodal proteins in control or KIF5AC double knockdown. Data are mean \pm SEM; $n=20$ to 24 neurons per condition from $n=3$ independent experiments. Student's two-tailed unpaired t-test (*, $p < 0.05$; **, $p < 0.01$; and ***, $p < 0.001$). The difference of puncta distribution between proteins across all types of movement was assessed using Chi-squared test (see Table S2 for exact p -values).

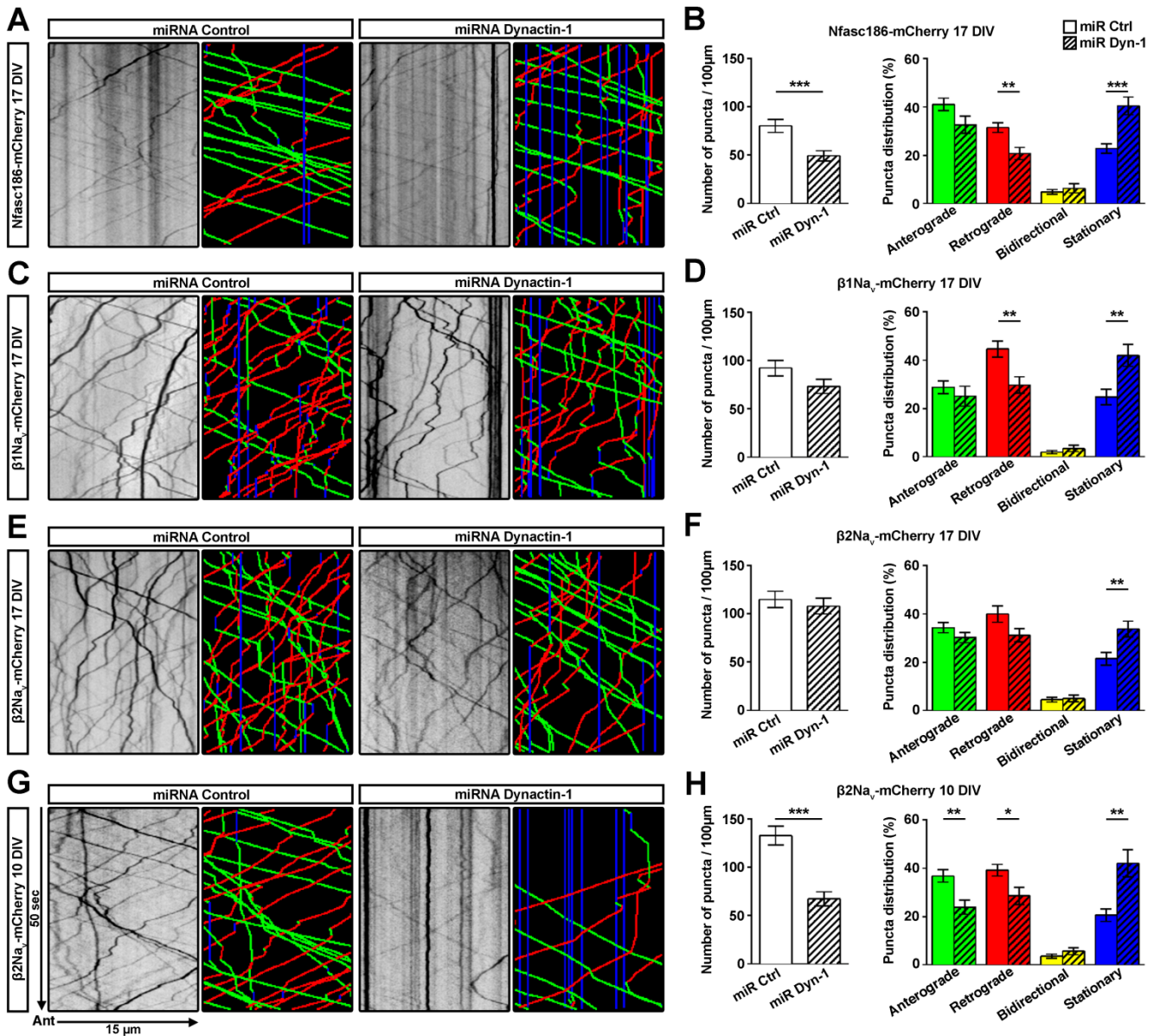


Figure 3. Dynactin-1 loss of function impairs CAMs transport.

Hippocampal mixed cultures were co-transfected with control or Dynactin-1 miRNA together with Nfasc186-mCherry (A, B), $\beta 1Na_v$ -mCherry (C, D) or $\beta 2Na_v$ -mCherry (17 DIV: E, F; 10 DIV: G, H) expressing constructs. (A, C, E, G) Kymographs and corresponding tracks. (B, D, F, H) Mean number of nodal CAMs puncta and their distribution in control or Dynactin-1 knockdown. Data are mean \pm SEM; $n=18$ to 25 neurons per condition from $n=3$ independent experiments. Student's two-tailed unpaired t-test (*, $p < 0.05$; **, $p < 0.01$; and ***, $p < 0.001$). The difference of puncta distribution between proteins across all types of movement was assessed using Chi-squared test (see Table S2 for exact p -values).

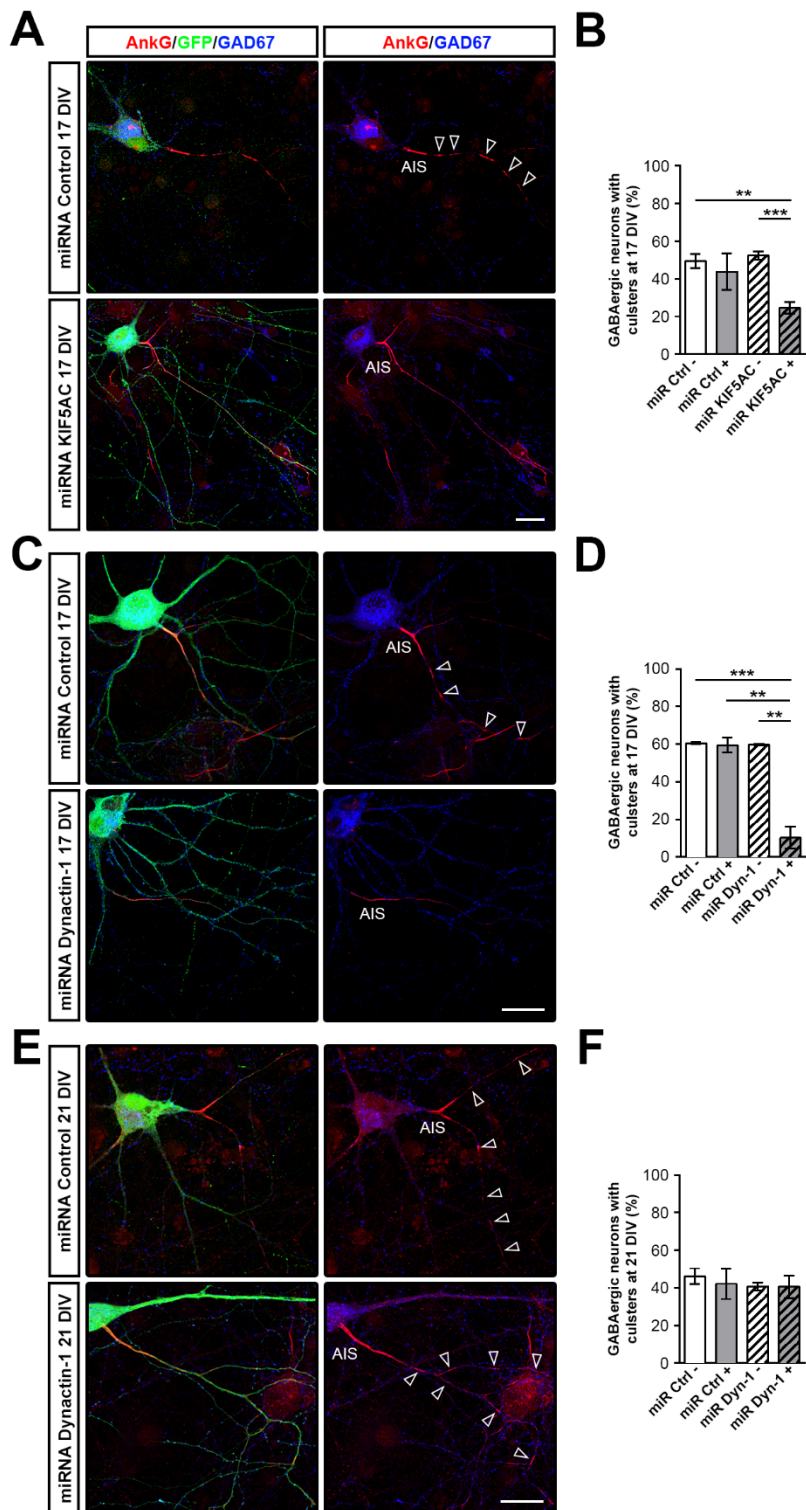


Figure 4. KIF5A, KIF5C and Dynactin-1 participate in early clusters assembly.

(A) The presence of early clusters (AnkG, red, arrowhead) is impaired in GABAergic neurons (GAD67, blue) expressing KIF5AC miRNA (GFP, green) compared to control condition (GFP, green) at 17 DIV, in contrast to the axon initial segment (AIS) which is preserved. Nodal marker expression (AnkG, red) becomes diffuse along the axon in KIF5AC miRNA condition. Scale bars, 25 μ m. (B) Quantification of GABAergic neurons with early clusters at 17 DIV in non-transfected neurons (miR Ctrl -/miR KIF5AC -) compared to transfected neurons with miRNA Control (miR Ctrl +) or miRNA KIF5AC (miR KIF5AC +) expressing constructs. (C) Early clusters (AnkG, red, arrowheads) are absent at 17 DIV in most GABAergic neurons (GAD67, blue) expressing Dynactin-1 miRNA (GFP, green) compared to control condition (GFP, green). (E) Early clusters (AnkG, red, arrowheads) are present at 21 DIV. Scale bars, 20 μ m. Quantification of GABAergic neurons with early clusters at 17 DIV (D) or 21 DIV (F) in non-transfected neurons (miR Ctrl - or miR Dyn-1 -) compared to transfected neurons (miR Ctrl + or miR Dyn-1 +). Mean \pm SEM of 3 to 4 independent experiments. Student's two-tailed unpaired t-test; *, $p < 0.05$; **, $p < 0.01$; and ***, $p < 0.001$ (see Table S2 for exact p -values).

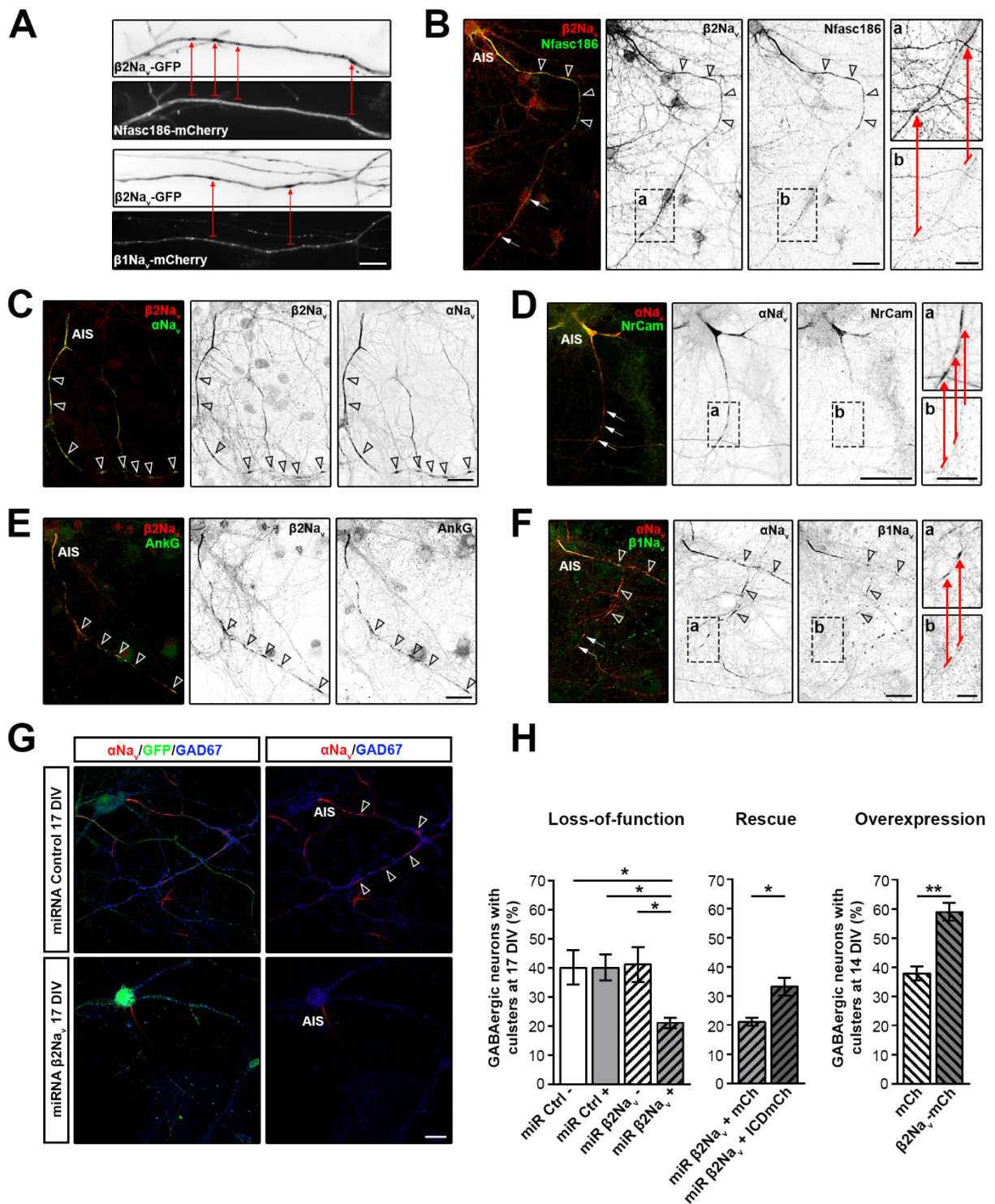


Figure 5. $\beta 2Na_v$ is a key player of early clusters initiation.

(A) Early axonal accumulation of $\beta 2Na_v$ -GFP (red arrows) in absence of Nfasc186-mCherry or $\beta 1Na_v$ -mCherry (red arrows counterpart) at 17 DIV in live cells. (B) $\beta 2Na_v$ (red) is enriched distally to the last cluster formed (arrowheads), prior to Nfasc186 accumulation (green, arrows). $\beta 2Na_v$ clusters (in red) always colocalize with αNa_v and AnkG (in green, C and E respectively, arrowheads). At 17 DIV, some distal clusters express αNa_v (red) without NrCAM or $\beta 1Na_v$ (in green, D and F, respectively, arrows). (G) Loss of early clusters (αNa_v , red, arrowheads) in GABAergic neurons (GAD67, blue) expressing $\beta 2Na_v$ miRNA (GFP, green) compared to control miRNA (GFP, green) at 17 DIV. AIS: axon initial segment. Scale bars, 5 μ m (A); 25 μ m (B-G); 10 μ m (a and b boxes). (H) Quantification of GABAergic neurons with clusters at 17 DIV in non-transfected neurons (miR Ctrl - or miR $\beta 2Na_v$ -) compared to transfected neurons (miR Ctrl + or miR $\beta 2Na_v$ +). At 17 DIV, GABAergic neurons transfected with the $\beta 2Na_v$ miRNA co-expressing mCherry (miR $\beta 2Na_v$ + mCh) or ICD-mCherry (miR $\beta 2Na_v$ + ICDmCh) show a partial rescue of clustering by ICD in absence of $\beta 2Na_v$. At 14 DIV, GABAergic neurons overexpressing $\beta 2Na_v$ -mCh show an increase in GABAergic neurons with early clusters compared to control condition (overexpression of mCherry alone). Mean \pm SEM of 3 independent experiments. Student's two-tailed unpaired t-test; *, $p < 0.05$; **, $p < 0.01$; and ***, $p < 0.001$ (see Table S2 for exact p -values).

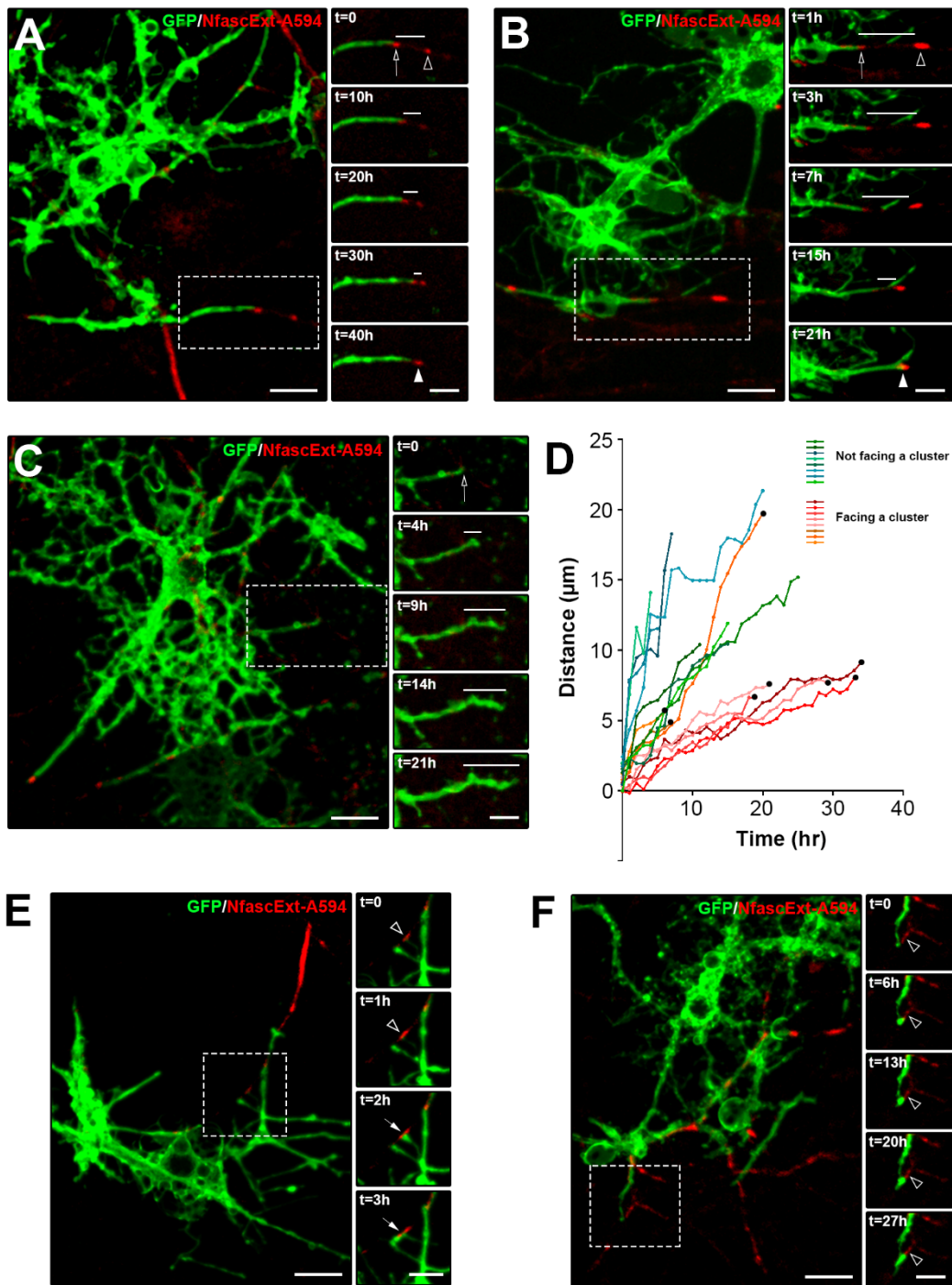


Figure 6. Live-imaging of early clusters fate during myelination *in vitro*

(A-C; E and F) For each live image, the boxed area is shown along time (right). Oligodendrocytes and myelin sheaths are visualized through GFP (green) and early clusters are revealed by live staining of the external epitope of Neurofascin (NfascExt-A594, red). (A, B) Fusion of a heminode (arrow) with an early cluster (arrowhead) during myelination (the line indicates the gap between the two structures at a given time). (C) Myelin growth along an axon without cluster at its vicinity (the line indicates myelin progression from the beginning (arrow) to the end of the imaging). (D) Distance covered by individual myelin sheaths along time. One color represents one individual myelin sheath with red-orange curves corresponding to individual myelin sheaths facing early clusters, while green-blue curves correspond to individual myelin sheaths without a cluster facing the progressing myelin tip. Black dots indicate the time point when a heminode and a cluster fuse. n=8 individual myelin sheaths for each condition (red/orange or blue/green curves). (A) is representative of the red pool of curves, while (B) shows the atypical high speed growth of myelin corresponding to the orange curve on (D). (E) An early cluster (red, arrowheads) is contacted by an oligodendrocyte (green, white arrows), which then starts to wrap the axon at its vicinity (E, F). A/B process : 10 out of 10 movies, C condition : repeated 8 times and E/F process : observed 7 times. Scale bar, 15 μm ; boxes, 10 μm .

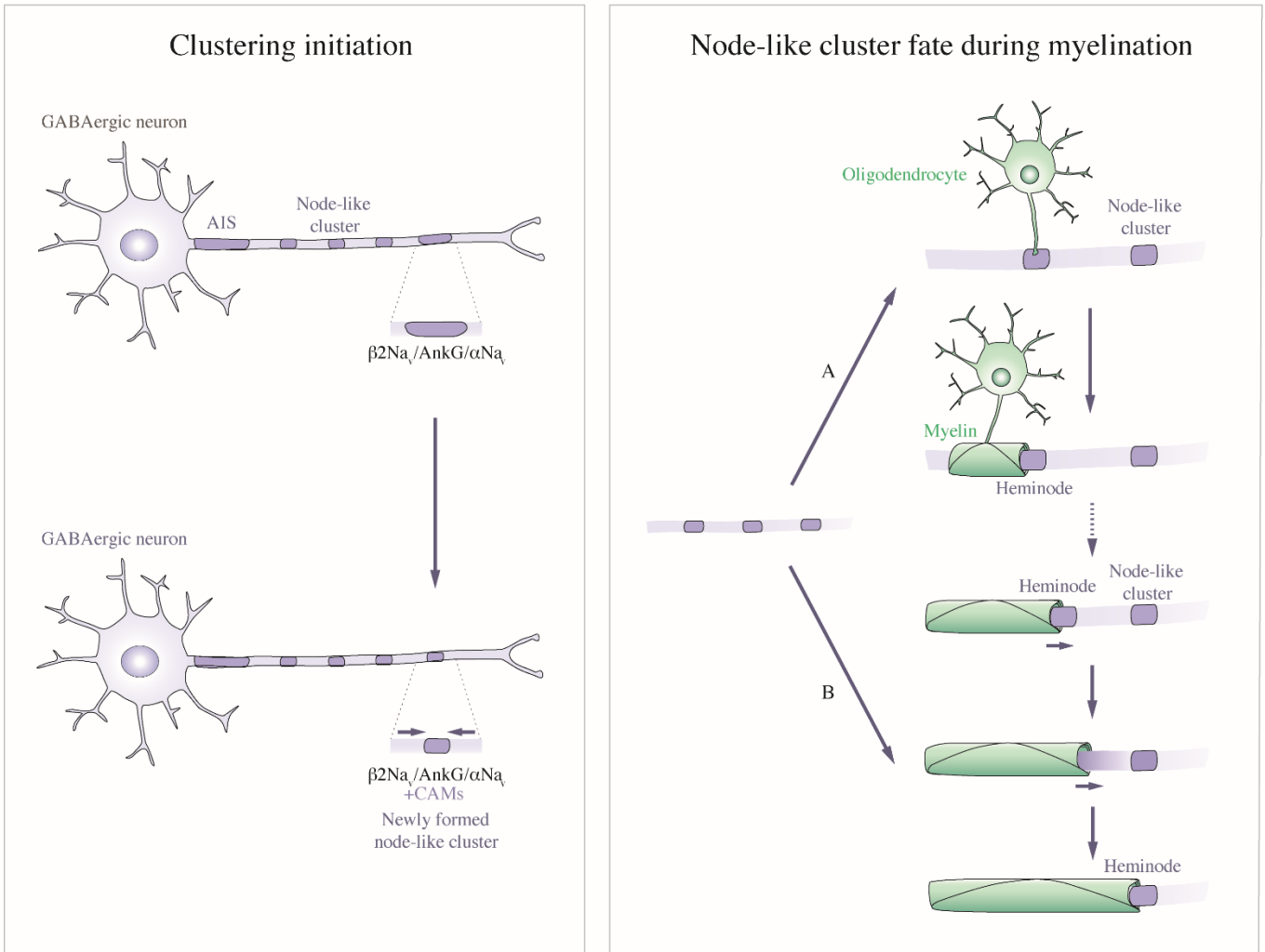


Figure 7. Model of node-like clustering initiation and fate during myelination.

(Left) Prior to myelination, a tripartite complex composed of $\beta_2\text{Na}_v$, αNa_v and AnkG accumulates distally to existing node-like clusters. Recruitment of other nodal CAMs to these enrichments are associated to their restriction and stabilization. **(Right)** At the onset of myelination, node-like clusters can be contacted by oligodendrocyte processes and act as localization signal to guide myelin initiation site, thus becoming heminodal structures **(A)**. When myelination proceeds, node-like structures participate in nodal assembly by fusion with heminodes **(B)**.